ELSEVIER

Multi-objective parameter estimation for simulating canopy transpiration in forested watersheds

D. Scott Mackay[a,*,1], Sudeep Samanta[a], Ramakrishna R. Nemani[b], Lawrence E. Band[c]

[a]Department of Forest Ecology and Management, Institute for Environmental Studies, University of Wisconsin—Madison, 1630 Linden Drive, Madison, WI 53706, USA
[b]School of Forestry, University of Montana, Missoula, MT 59812, USA
[c]Department of Geography, University of North Carolina—Chapel Hill, Chapel Hill, NC 27599, USA

Abstract

A Jarvis based [Philos. Trans. R. Soc. London, Ser. B 273 (1976) 593] model of canopy stomatal conductance was evaluated in context of its application to simulating transpiration in a conifer forest covered watershed in the Central Sierra Nevada of California, USA. Parameters influencing stomatal conductance were assigned values using Monte Carlo sampling. Model calibration was conducted by evaluating predicted latent heat fluxes against thermal remote sensing estimates of surface temperature. A fuzzy logic approach was used to select or reject simulations and form a restricted set of ensemble parameter solutions. Parameter estimates derived from the ensembles were evaluated using theory on how stomatal conductance regulates leaf water potential to prevent runaway cavitation. Canopy level parameters were found to be sufficient for predicting hydraulically consistent transpiration when soils were well watered. A rooting length parameter controlling the amount of plant available water was a sufficient addition to the parameter set to predict hydraulically consistent transpiration when soil moisture stress was occurring. Variations in maximum stomatal conductance among different hillslopes within the watershed were explained by a light threshold parameter. The results demonstrate that the Jarvis model can be reliably parameterized using thermal remote sensing data for estimating transpiration in meso-scale watersheds.
© 2003 Elsevier Science B.V. All rights reserved.

Keywords: Stomatal conductance; Simulation model; Parameter estimation; Transpiration; Thermal remote sensing

1. Introduction

Spatially variable transpiration is a major component flux simulated by distributed land surface process models. Although there is a scarcity of observational data to directly support large-scale simulation of canopy transpiration from forests, many models operating from watersheds to global scales (Running and Coughlan, 1988; Aber and Federer, 1992; Band et al., 1993; Running and Hunt, 1993; Famiglietti and Wood, 1994; Wigmosta et al., 1994; Vertessy et al., 1996; Foley et al., 1996, 2000; Mackay and Band, 1997; Sellers et al., 1997; and others) simulate transpiration using some form of the Penman–Monteith combination equation (P–M)

* Corresponding author. Tel.: +1-608-262-1669; fax: +1-608-262-9922.
E-mail address: dsmackay@facstaff.wisc.edu (D.S. Mackay).
[1] Present address: Department of Geography, 105 Wilkeson Quad, University at Buffalo, Buffalo, NY 14261. Tel.: +1-716-645-2722; fax: +1-716-645-2329.

(Monteith, 1965) and one of several empirical models of stomatal conductance (Jarvis, 1976; Lohammar et al., 1980; Ball et al., 1987). Although there are numerous sources of uncertainty in P–M models, the unknowns associated with stomatal conductance are most critical for understanding vegetation responses to climate change and land use pressures. Mackay et al. (2003) show that Jarvis-type models mimic the stomatal regulation of leaf water potentials in a detailed canopy model operating at sub-daily time resolution, with in situ micrometeorological measurements and sap flux data for calibration. The study by Mackay et al. (2003) was limited to four forest stands each approximately 30 m in diameter. To extend the applicability of their approach to watershed or global scales necessitates finding tractable data sources and more moderate model detail.

One potential source of data for characterizing the state of a land surface is thermal remote sensing. Thermal remote sensing data is a measure of surface temperature, which is a function of energy partitioning and surface resistance. Foliage temperature has been shown to relate to soil moisture, plant moisture stress, and transpiration (Idso et al., 1978; Jackson et al., 1981). This has led to numerous applications of thermal remote sensing to study canopy processes (Goward et al., 1985; Pierce and Congalton, 1988; Holbo and Luvall, 1989; Nemani and Running, 1989; Kustas et al., 1994; Carlson et al., 1995; Anderson et al., 1997; Franks and Beven, 1997; Bastiaanssen et al., 1998; Norman et al., 2000). These methods have been successful using very different approaches. Representative approaches include modeling with detailed ground flux measurements and sub-daily remote sensing measurements to look at thermal inertia (Anderson et al., 1997; Norman et al., 2000), limiting the analysis to large-scale remote sensing with strong moisture gradients and well-coupled forest canopies (Nemani and Running, 1989), or calibrating a model using Monte Carlo analysis with contrasting vegetation types (Franks and Beven, 1997).

In this paper, the latter two approaches are combined to evaluate a Jarvis-type model as used within the Regional Hydro-Ecological Simulation System (RHESSys) (Band et al., 1993) applied to a meso-scale watershed in the Central Sierra Nevada. RHESSys has been and continues to be applied successfully in numerous forested watershed studies

(Band et al., 1996; Creed et al., 1996; Watson et al., 1996; Mackay and Band, 1997; White et al., 1998; Baron et al., 2000; Tague and Band, 2001; Zhu and Mackay, 2001; Samanta and Mackay, 2003). Its ability to predict stream flow, nitrate export, and responses to forest manipulation and road construction are documented in these studies. However, neither RHESSys nor any model like it has been tested for consistent spatial transpiration. The question is whether RHESSys can produce transpiration at a watershed scale that is consistent with plant water relation theory. Significant progress has recently been made in the understanding of hydraulic limitations to canopy transpiration. These limitations have helped in constraining parameters for a Jarvis-type model at the stand level (Mackay et al., 2003). It is hypothesized that transpiration estimates can be similarly evaluated through calibration of Jarvis-type parameters controlling stomatal conductance at larger spatial scales and on daily time-step, by comparing model predictions and thermal remote sensing estimates of surface energy partitioning. Rejecting this hypothesis would mean that the model is either deficient with respect to processes such as soil water distribution, the Jarvis-type model is a poor approximation to the stomatal conductance at daily time-steps or at larger spatial scales, or the combination of data and models used in the analysis are insufficient to resolve the underlying regulation of leaf water potential by stomata, which ultimately affects energy partitioning.

The paper is organized as follows. First, a summary of the most relevant elements of plant water relations are presented to build a framework for relating the Jarvis-type stomatal conductance model to tree hydraulic theory. This is followed by the methods, which describes an automated calibration based on Samanta and Mackay (2003) and restricted using the tree hydraulic theory (Mackay et al., 2003). Relevant details on RHESSys are presented, followed by the analysis of thermal remote sensing imagery, results, discussion, and conclusions.

2. Plant water relations and the Jarvis model of stomatal conductance

Canopy transpiration from forests is generally simulated with the well-known P–M 'big leaf' model

(Monteith, 1965). A key variable in P–M is canopy conductance, which is determined by the product of stomatal conductance, g_S and leaf area, L. Models of stomatal conductance address one or more environmental (extrinsic) and physiological (intrinsic) conditions of the leaf stomata. There are two distinct empirical models of stomatal conductance: Ball–Berry (Ball et al., 1987; Leuning et al., 1995) and Jarvis (Jarvis, 1976; Lohammar et al., 1980). The Ball–Berry model emphasizes the rate of carbon assimilation in controlling stomatal conductance, but places little emphasis on water supply and demand. Jarvis models more directly address water supply and demand through soil water limitation and atmospheric vapor pressure deficit functions, respectively. Jarvis-type models have the general form:

$$g_S = g_{Smax} \prod f_i, \tag{1}$$

where g_{Smax} is a theoretical maximum stomatal conductance under assumed optimal environment and leaf conditions. A series of multiplicative functions of environmental factors (f_i) are applied to reduce actual leaf level stomatal conductance from the theoretical maximum level. Typically, one function considers the stomatal sensitivity, δ, to atmospheric vapor pressure deficit, D. The g_{Smax} parameter can vary widely among and within species (Kelliher et al., 1995; Ewers et al., 2001) and δ is widely believed to increase with maximum stomatal conductance (Jarvis, 1976, 1980; McNaughton and Jarvis, 1991; Monteith, 1995; Saliendra et al., 1995; Oren et al., 1999). Low vapor pressure gradient conditions favor stomatal control by assimilation rate, but as D increases stomata close to reduce water loss (Ball et al., 1987; Monteith, 1995; Saliendra et al., 1995; Yong et al., 1997). One advantage of the Jarvis model for water flux estimates is that it directly addresses plant response to D. This suggests that it operates best when the rate of water loss is high and, hence, hydrologically significant. Furthermore, recent developments in plant hydraulic theory have been successfully combined with Jarvis models (Oren et al., 1999; Ewers et al., 2000) and tested in diurnal canopy models on a range of forest species (Mackay et al., 2003).

Eq. (1) is a proxy for the hydraulic functioning of the soil–plant–atmosphere continuum. In the absence of stomatal control, a high rate of water loss from a plant leads to a rapid decline in leaf water potential. This increases the risk of hydraulic failure in the plant (Sperry et al., 1998; Oren et al., 1999; Ewers et al., 2000). The relationship between stomatal conductance and water potential can be expressed with the steady-state assumption and Darcy's law (Tyree and Ewers, 1991; Ewers et al., 2000):

$$G_S = K_L/D(\Psi_S - \Psi_L - h\rho_w g), \tag{2}$$

where G_S is canopy average leaf level stomatal conductance, K_L is leaf-specific whole-plant hydraulic conductance, Ψ_S and Ψ_L are bulk soil and leaf water potentials, respectively, and $h\rho_w g$ is the gravitational potential for a plant of height h. K_L declines with water potential due to soil drying, cavitation in the xylem, and other factors. As K_L declines a further drop in water potential is needed to sustain increasing transpiration (E_C) per unit leaf area (L). This drop in water potential further reduces K_L as a positive feedback. Once the maximum safe transpiration rate is exceeded then runaway cavitation ensues. Runaway cavitation refers to K_L being driven to zero causing hydraulic failure and possible plant mortality (Tyree and Sperry, 1988). Eq. (2) also captures the well-known fact that G_S is inversely proportional to D (Jarvis, 1976; McNaughton and Jarvis, 1991), which drives down stomatal conductance even when plants are well watered in the soil. This is shown conceptually in Fig. 1. G_S is further shown to be sensitive to increasing D in proportion to some maximum conductance, g_{Smax}, or its proxy (Oren et al., 1999):

$$G_S = G_{Sref} - m \ln D, \tag{3}$$

where G_{Sref} is a substitute for g_{Smax} defined at $D = 1$ kPa and $m = dG_S/d \ln D$ is the sensitivity of stomatal conductance to increasing D. In Eq. (3), G_{Sref} is typically near linearly related to the sensitivity of stomatal conductance to D. Based on a large amount of porometry and sap flux data, Oren et al. (1999) have shown that $m \approx 0.6G_{Sref}$ applies universally to all species whose stomata regulate leaf water potential to just prevent runaway cavitation.
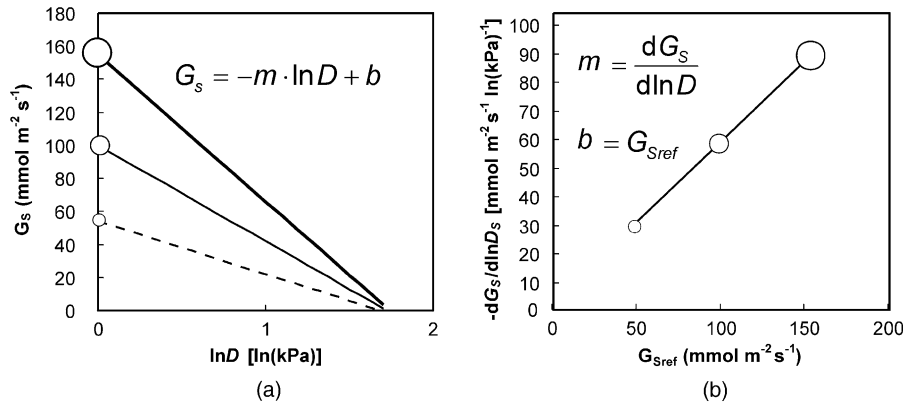
Fig. 1. The rates of stomatal closure (lines) in response to vapor pressure deficit are proportional to the maximum stomatal conductances (circles) (a), have been shown to result in all species that just regulate leaf water potential to prevent runaway cavitation to lie along a line representing the stomatal sensitivity to vapor pressure deficit versus reference conductance at 1 kPa ($\ln D = 0$).

3. Methods

3.1. Overview of the model parameterization approach

In this paper, two distinct stages of parameter estimation are used. The first stage of parameter estimation follows a traditional automated calibration. Many simulations are run in which parameters affecting stomatal conductance are assigned values using Monte Carlo sampling. Each simulation result is then evaluated by applying a linear least-squares regression between simulated evaporative fraction from RHESSys and surface temperature from thermal remote sensing data. For each least-squares regression, the coefficient of determination (or R^2) is calculated. The R^2 is then considered a fuzzy measure of the goodness-of-fit for its respective simulation result. The set of R^2 measures for all simulations is considered a fuzzy set (Samanta and Mackay, 2003). An information-theoretic tool is then applied to the fuzzy set to form a restricted set in which only 'good' simulations retained. A restricted set is used as an ensemble solution in the second stage of parameter estimation. A separate ensemble solution is produced for each areal unit simulated by RHESSys, and in the present work these areal units are hillslopes.

The second stage of parameter estimation applies the universal line represented by Eq. (3) and shown in Fig. 1. For each ensemble δ is related to g_{Smax}. When a δ/g_{Smax} combination falls on the universal line, it is

assumed to be consistent with plant hydraulic theory. Otherwise, it is considered inconsistent with the theory. To be consistent with the conventions of Oren et al. (1999), Jarvis parameters (δ and g_{Smax}) are mapped into their respective universal line counterparts (m and G_{Sref}). For the remainder of this paper the use of δ and g_{Smax} will be restricted to discussion of model function, not plant physiology. Discussion of plant physiology will use m and G_{Sref}.

3.2. Stage 1: model-independent automated parameterization

An objective automated parameter estimation framework (Samanta and Mackay, 2003) was used to calibrate RHESSys. The approach is based on a number of hydrologic parameter estimation schemes (Kuczera, 1982, 1983; Sorooshian and Gupta, 1983; Spear and Hornberger, 1990; van Stratten and Keesman, 1991; Klepper et al., 1991; Binley and Beven, 1991; Melching, 1995; Kuczera and Parent, 1998; Gupta et al., 1998; Yapo et al., 1998; Boyle et al., 2000). It combines Monte Carlo sampling and measures of uncertainty derived from information processing. One information-theoretic expression of uncertainty in information processing is the Hartley (1928) Function:

$$H(A) = \log_2 |A|, \tag{4}$$

where $H(A)$ is the Hartley Function for a finite set, A, and $|A|$ is its cardinality. Eq. (4) is a measure of

the non-specificity arising from an inability to identify a unique solution. Higher values of $H(A)$ represent greater non-specificity. If A represents a set of retained simulations, each defined by a simulation model and its parameters, then $H(A)$ is the non-specificity associated with this equifinal (Beven and Binley, 1992) set of simulations.

The above notion of the non-specificity of a set of simulations can be extended to incorporate measures of model fitness. If each simulation has an associated measure of fitness or degree of fit to some observation data, then the acceptable set of models can be considered a fuzzy set (Zadeh, 1965). For a fuzzy set, F, defined by a measurement of fitness, $f(x_i)$, for member x_i within the domain, X, of all simulations, a fuzzy logic measure of the non-specificity of F is (Higashi and Klir, 1982; Klir and Wierman, 1998):

$$U(F) = \int_0^{h(F)} \log_2 |^\alpha F| \mathrm{d}\alpha + (1 - h(F))\log_2|X|, \quad (5)$$

where $U(F)$ is the U-uncertainty associated with F, $|^\alpha F|$ is the cardinality of an α-cut of F (i.e. the number of members that remain in the set if all members with a degree of fitness less than α are removed from F), $h(F)$ is the height of F (or maximum degree of fitness in F), and $|X|$ is the cardinality of the universal set (i.e. the population of simulations). A discrete approximation of Eq. (5) is given by

$$U(r) = \sum_{i=2}^{n} (r_i - r_{i+1})\log_2 i + (1 - r_1)\log_2 n, \quad (6)$$

where r is the ordered possibility distribution (Zadeh, 1978) derived from the fuzzy set F and r_{n+1} is assumed to be 0. Fig. 2 shows two typical possibility distributions relating $f(x_i)$, which is the goodness-of-fit measure, and $|^\alpha F|$, as well as the physical meaning of the α-cut. Both distributions are shown to have an α-cut of about 0.6, at which they yield very different cardinalities. Relations that are skewed towards the low end, and thus have only a few high $f(x_i)$ models, are better than relations having too many high $f(x_i)$ values. The ideal distribution of simulations relation has one with $f(x_i) = 1.0$ and all others with $f(x_i) = 0.0$. This would represent a case where the best simulation is uniquely identifiable. For numerous reasons, including model flaws, parameter trade-offs, and limitations of objective functions, hydrologic
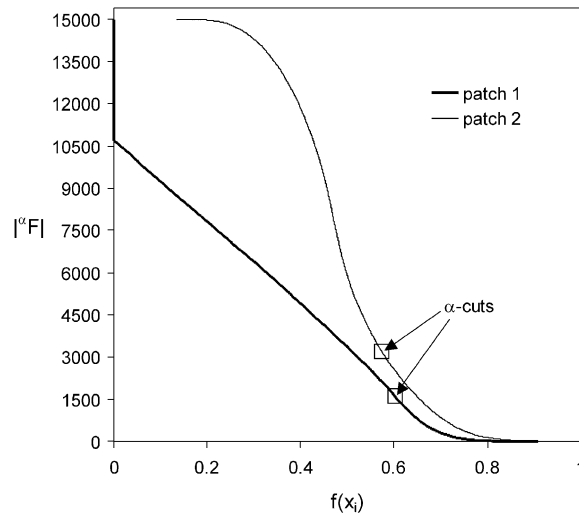
Fig. 2. Shown is an illustration of the types of possibility distributions that are commonly obtained from the U-uncertainty analysis. The plots represent the relationship between cardinality on the y-axis and value returned by some model evaluation objective function applied to simulations of two hypothetical landscape patches. Shown are the α-cuts obtained by minimizing $|U(r) - \log_2 k|$. It is important to note that similar α-cuts may be obtained from different sets of simulations in which the retained model sets have very different cardinalities.

models do not satisfy this ideal (Oreskes et al., 1994; Mackay and Robinson, 2000).

It is tempting to set the α-cut at such a level that only one simulation is retained. This is the traditional approach to model calibration. However, an objective criterion provides a better way to define the α-cut to form a restricted set from the fuzzy set (Samanta and Mackay, 2003). Initially, this α-cut should be selected with caution. On the one hand, useful information in the fuzzy set may be lost if an arbitrarily high α-cut is selected. An arbitrarily high α-cut may also admit a false sense of specificity to the identified model parameters. On the other hand, an arbitrarily low α-cut may include too many simulations of poor quality. Information Theory presents a rich set of tools for extracting the full information content of a fuzzy set. One tool, the Principle of Uncertainty Invariance (Klir and Wierman, 1998), transforms a fuzzy set into a 'crisp' restricted set that approximates the respective fuzzy set by virtue of having the same U-uncertainty. The α-cut is chosen at the kth element of the ordered possibility distribution at which $|U(r) - \log_2 k|$ is minimized. As an illustration, consider the ordered

fuzzy set $F = \{0.9, 0.8, 0.8, 0.7, 0.6, 0.4, 0.1, 0.1\}$. It is possible to calculate $|^{\alpha}F| = 4.4$ as the sum of fuzzy memberships in the set and $U(r) = 2.2$ as its associated U-uncertainty. The size of the restricted set is determined by equating the U-uncertainty of the fuzzy set (Eq. (6)) to the Hartley Function (Eq. (4)) for the desired crisp set. The value of k (5 in this example) is the required cardinality of the restricted set, which means that the top five elements in F are retained and the α-cut is placed at 0.6. An advantage of this approach is that the selection of the α-cut is not subject to interpretation or modification as the goals of a modeling exercise change. A disadvantage of the approach is that it does not consider intuition about the physical system, which is an essential part of parameter estimation (Boyle et al., 2000). However, once an objective solution set has been established, further analysis can be applied to determine if a more refined solution can be found. In this paper, a simple averaging of the respective parameter values from the restricted sets is tested by evaluating the degree to which the chosen parameters for a Jarvis-type model are consistent with the plant hydraulic theory relationships (Refer to Section 2). The Jarvis-type model and its parameterization are described in Section 3.3.

3.3. Stage 2: parameterization specific to RHESSys canopy transpiration

RHESSys combines forest canopy gas exchange processes, soil moisture balance, and lateral saturated through flow (Band et al., 1993). It represents watersheds as collections of hillslopes, which are themselves divided into elevation zones for adiabatic adjustment of air temperature, T_a. Each elevation zone is segmented into hydrologically uniform patches defined using the TOPMODEL topography and soil index (TSI) (Beven and Kirkby, 1979; Beven, 1986; Sivapalan et al., 1987; Quinn et al., 1995). All vertical fluxes, including evapotranspiration, are calculated at the patch level. Complete details on the design and implementation of RHESSys are provided in previous publications (Band et al., 1993; Mackay and Band, 1997; Mackay, 2001). This section focuses on model components that directly affect the calculation of stomatal conductance. Leaf level stomatal conductance (m s^{-1}) is determined (from Eq. (1)) in

RHESSys as:

$$g_S = g_{Smax}g_1(D)g_2(\Psi_L)g_3(Q), \qquad (7)$$

where

$$g_1(D) = 1 - \delta D \qquad (8)$$

and δ [(kPa)$^{-1}$] has been previously defined as the sensitivity of stomatal conductance to D. From the earlier discussion it should be apparent that Eq. (8) is a surrogate for stomatal response to the rate of water loss from the canopy, which is strongly related to D in well-ventilated forest canopies (McNaughton and Jarvis, 1991). This can be interpreted in the terms used in Eq. (4) by mapping g_{Smax} and δ into G_{Sref} and $dG_S/d \ln D$, respectively. The g_{Smax} parameter represents a theoretical optimal stomatal conductance under ideal conditions (i.e. low D, sufficient light, moderate temperature, well-watered soils). Following Eq. (8) $g_S \equiv g_{Smax}$ at $D = 0$ kPa. It is not possible to measure g_S at $D = 0$ kPa, and so g_{Smax} is transformed into G_{Sref} (at $D = 1$ kPa as defined by Oren et al. (1999)) as follows:

$$G_{Sref} = g_{Smax}(1 - \delta). \qquad (9)$$

Similarly δ is converted into m as follows:

$$m = dG_S/d \ln D = g_{Smax}d\delta/d \ln D, \qquad (10)$$

in which the derivative is calculated by finite-difference at two values of D (Mackay et al., 2003). The other functions (g_2 and g_3) in Eq. (7) are not modified from their standard expressions. Stomatal conductance is further reduced using a hyperbolic function of leaf water potential, Ψ_L, which is assumed to be equal to pre-dawn soil water potential calculated using a van Ganuchten (1980) formulation parameterized using Brooks and Corey (1964) soil hydraulic parameters. Stomatal conductance is reduced linearly with the ratio of absorbed radiation in the canopy to a minimum threshold radiation, Q_{min}.

RHESSys calculates soil water potential within a depth of soil defined by plant rooting length, R_L. R_L is varied spatially to account for two competing controls on water supply: (1) the tendency for capillarity to recharge a drying rooting zone when there is a shallow perched water table, and (2) the need for sufficient R_L to support the water demand associated with a given leaf area index, L (Grier and Running, 1977; Gholz, 1982), or, equivalently,

the root-shoot ratio. R_L is spatially co-varied with L and S (Mackay, 2001), expressed for a given patch, i, of uniform TSI within hillslope, h, as

$$R_{L,i} = R'_h L_{h,i} f_h(S_{h,i}), \tag{11}$$

where R'_h is intrinsic rooting length (per unit $L_{h,i}$) for a mesic site on h (m), $f_h(S_{h,i})$ is a function, which, through dimensional analysis, describes relative soil saturation deficit at i with respect to average soil saturation deficit within h, and $L_{h,i}$ is leaf area index defined at i on h (m^2 m^{-2}). Eq. (11) accounts for higher water demand environments (e.g. south-facing slopes, high temperatures) by increasing R'_h. Furthermore, high $L_{h,i}$ requires proportionally deeper roots to supply adequate water to the canopy. Sites with low saturation deficits do not require deep roots, and roots cannot survive long in a shallow water table (Larcher, 1995).

The derivation of $f_h(S_{h,i})$ is based on elements of TOPMODEL (Beven, 1986; Beven and Kirkby, 1979; Sivapalan et al., 1987). Profile saturation deficit is scaled from hillslope facet average saturation deficit as

$$\langle S_h \rangle - S_{h,i} = m_h(\text{TSI}_{h,i} - \langle \text{TSI}_h \rangle), \tag{12}$$

where $\langle S_h \rangle$ is mean saturation deficit for h (m), $S_{h,i}$ is saturation deficit of patch i of h (m), m_h is a parameter that describes the rate of decay of saturated hydraulic conductivity through a soil profile in hillslope h, $\text{TSI}_{h,i}$ is topography–soils index at patch i of hillslope h (m), and $\langle \text{TSI}_h \rangle$ is hillslope average topography–soils index (m). $\text{TSI}_{h,i}$ is calculated as follows:

$$\text{TSI}_{h,i} = \ln\left(\frac{a_{h,i} t_h}{t_{h,i} \tan \beta_{h,i}} \right), \tag{13}$$

where $a_{h,i}$ is accumulated upslope drainage area per unit contour width (m), $\beta_{h,i}$ is local topographic slope, $t_{h,i}$ is local soil transmissivity (m day^{-1}), and t_h is hillslope average transmissivity (m day^{-1}). Eq. (12) can be conditionally expanded to describe $S_{h,i}$ as

a function of $\langle S_h \rangle$:

$$S_{h,i} = \begin{cases} = \langle S_h \rangle, & \dfrac{\langle \text{TSI}_h \rangle}{\text{TSI}_{h,i}} = 1 \\[2ex] < \langle S_h \rangle, & \dfrac{\langle \text{TSI}_h \rangle}{\text{TSI}_{h,i}} < 1 \\[2ex] > \langle S_h \rangle, & \dfrac{\langle \text{TSI}_h \rangle}{\text{TSI}_{h,i}} > 1 \end{cases} \tag{14}$$

From Eq. (14) the relative saturation deficit can be determined from hillslope average conditions with the dimensionless form:

$$f_h(S_{h,i}) = \frac{\langle \text{TSI}_h \rangle}{\text{TSI}_{h,i}}. \tag{15}$$

Substituting Eq. (15) into Eq. (11) gives a relation for scaling rooting length along joint moisture and leaf area gradients within a hillslope,

$$R_{L_{h,i}} = R'_h L_{T_{h,i}} \frac{\langle \text{TSI}_h \rangle}{\text{TSI}_{h,i}}. \tag{16}$$

The parameter, R'_h, can be modified to linearly scale the depth of soil available for plant access to water.

3.4. Evaluation data set

Data to test the Jarvis-based model in RHESSys was obtained from the Onion Creek Experimental Forest, a 10 km^2 watershed located along the crest of the Central Sierra Nevada of California. Annual precipitation averages 1300 mm, of which 90% falls as snow between October 1 and March 31. Relief within the watershed is about 1000 m, with the highest elevation occurring at ca. 2600 m above mean sea level. Soils are generally poorly developed loamy sands overlying highly permeable rhyolitic ash and latite deposits (MacDonald, 1987). The soils and underlying parent material have a high storage capacity producing long lags in the baseflow recession (MacDonald, 1986). Vegetation cover is predominantly mature to old-growth mixed needle-leaf conifers. The dominant tree species in the basin are White Fir (*Abies concolor*), Red Fir (*Abies magnifica*), Sugar Pine (*Pinus lambertiana*), Jeffrey Pine (*Pinus jeffreyi*), Lodgepole Pine (*Pinus contorta*), and Incense Cedar (*Calocedrus decurrens*). Cedar

generally occupies lower elevations, pine at mid-elevations, and fir at higher elevations.

Radiometric thermal data was acquired with the NASA-Ames Research Center's airborne Thematic Mapper Simulator (TMS), a Daedelus scanner flown aboard a U-2 aircraft, on July 2 and August 6, 1985. The image data was collected in conjunction with field-measured surface temperature and soil moisture (Pierce and Congalton, 1988; MacDonald, 1989). On July 2, soil moisture measurements in the watershed showed soil moisture levels between field capacity and saturation. On August 6 the soils were well below field capacity and approaching wilting point in some plots (MacDonald, 1989). The TMS images were collected at approximately solar noon at a flying height commensurate with a sensor resolution of 30 m (or 0.09 ha per observation). The flight lines were centered over Onion Creek to avoid off-nadir geometry problems, allowing for relatively accurate co-registration of the TMS with a Landsat Thematic Mapper 4 (TM) scene (RMS error < 15 m). Sensor radiance values, r, were converted to kinetic temperatures, t, with the following regression and parameters (Table 1) obtained from black-body radiation sensor calibration reference plates, atmospheric correction, and ground control within Onion Creek (Pierce and Congalton, 1988):

$$T_s = \frac{t_{max} - t_{min}}{r_{max} - r_{min}}(10r - r_{min}) + t_{min}. \quad (17)$$

No adjustment was made for variations in surface emissivity, as the range of cover types in Onion Creek (occasional bare soil to predominantly dense conifer canopy) should have emissivities of 0.9–0.95, which translates into 1–3% error when inverting the Stefan–Boltzmann Equation to convert from radiant to kinetic temperature.

Kinetic temperatures are influenced by a number of other factors in complex topography. These factors include stomatal, boundary and aerodynamic

resistances, which effect latent and sensible heat transfer; meteorological differences, such as cloud cover and air temperature between flight dates; temperature lapse with elevation; land surface–sun geometry; and forest canopy density. Meteorological data was obtained from the Central Sierra Snow Lab. Fig. 3 shows daily temperatures (maximum and minimum) and precipitation for the period beginning before the July 2 TMS scene and ending after the August 6 scene. Both dates show similar daily high and low temperatures, and clear skies following several days with no precipitation. Aerodynamic conductance was assumed high (set at 0.2 m s^{-1}) for the dense, conifer needle-leaf forests covering much of Onion Creek. TM data was used to derive leaf area index (LAI) using ground-based calibration and image processing procedures described in Nemani

Table 1
Black body reference plate regression parameters used in Eq. (14) to convert TMS pixel values to radiant temperatures

Date	t_{max}	t_{min}	r_{max}	r_{min}
July 2	32.21	8.18	149.00	105.00
August 6	32.32	8.49	150.00	110.00
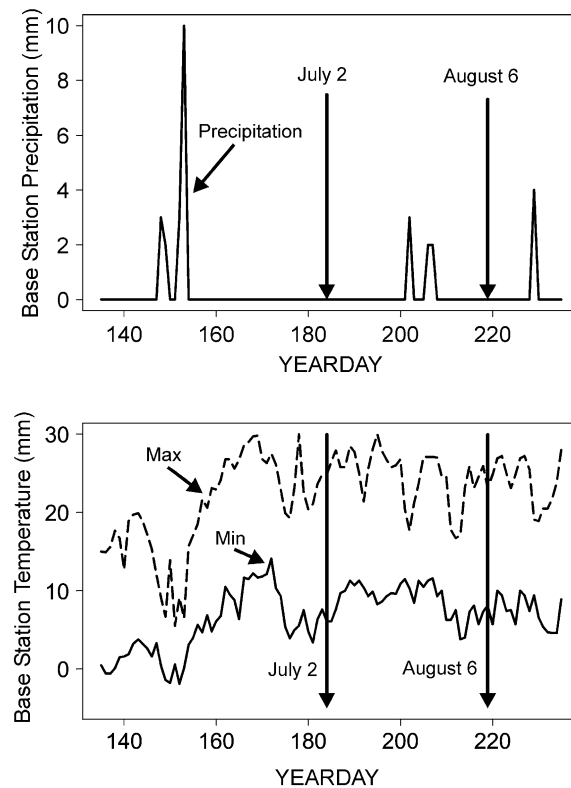
Fig. 3. This shows the meteorological conditions spanning the period around the two selected dates (July 2 and August 6) for the TMS imagery. Note that both dates occur during a dry period with no recent rainfall, and with similar maximum and minimum temperatures.

et al. (1993). A USGS 30 m digital elevation model (DEM) was used to identify hillslopes that account for variability in land surface–sun geometry, and elevation bands that account for temperature lapse rates. A digitized soils map was acquired from the US Forest Service, and used for soil parameterization of RHESSys. Table 2 summarizes topography, vegetation, and other hillslope facet mean properties of Onion Creek, partitioned into 25 hillslope partitions (Liang and Mackay, 2000).

A separate objective function was used for each TMS scene for each model. Linear least-squares regression between evaporative fraction, $\sigma = \lambda E_C/Q$, and surface departure from air temperature, $dT = T_s - T_a$ was used to evaluate model fitness. The reason for using σ is that it remains nearly constant during the mid-day period (Crago, 1996; Crago and Brutsaert, 1996) and so it is less likely to be sensitive

to short-term changes in micrometeorological conditions than is latent heat flux alone. Furthermore, whereas λE_C and Q both give a non-linear fit to surface temperature data due to their asymptotic response with leaf area index through the Beer–Lambert Equation, their ratio is close to linear. As a requirement for using TMS imagery collected at a single point in time at solar noon, it is necessary to assume that midday dT is correlated with daily E_C at a given aerodynamic conductance (Seguin and Itier, 1983; Carlson et al., 1995). Furthermore, it was assumed that soil heat flux had a minimal influence on canopy temperature given the high leaf area (Carlson et al., 1995). Finally, residuals derived from the best model for each hillslope facet for each TMS scene were checked for trends. There were no visible trends in the residuals that would suggest a linear fit was inappropriate.

Table 2
This shows a summary of the average properties of all hillslopes in the Onion Creek watershed partitioning. Number of zones refers to the number of elevation zones used to capture within-hillslope adiabatic temperature lapse rates. Each zone represents an increment of 30 m altitude, such that a hillslope with 20 zones has an elevation range of about 600 m

Hillslope identifier	Area (ha)	Aspect (°)	Elevation (m)	Slope (°)	L ($m^2\,m^{-2}$)	$\langle TSI_h \rangle$ (m)	Number of zones
1	30.6	143.1	1791.3	11.3	8.59	8.2	11
2	34.4	265.1	1804.3	10.2	9.02	7.26	12
3	64.7	111.1	1896.4	12.8	9.17	8.11	10
4	21.0	264.4	1834.1	9.3	9.13	6.67	4
5	11.6	98.3	1917.0	13.6	8.98	7.69	9
6	1.9	159.2	1864.9	15.0	8.92	8.63	3
7	30.1	91.6	2041.3	10.2	9.11	7.47	11
8	24.5	187.5	2063.9	11.2	10.57	6.83	12
9	82.7	133.3	2108.7	15.5	8.53	7.12	15
10	43.7	219.8	2074.8	13.7	8.43	7.08	15
12	2.7	293.3	1851.1	9.6	7.89	6.87	3
13	159.2	119.6	2060.7	16.8	7.46	7.13	18
14	92.2	238.6	2091.8	18.6	8.77	6.99	19
15	7.9	206.9	1880.2	3.2	7.75	10.6	3
16	67.9	283.7	1958.0	12.7	8.65	7.59	12
17	42.7	140.0	2130.7	19.3	6.50	6.57	17
18	54.1	229.3	2144.2	18.3	7.29	6.71	18
19	6.8	182.6	1972.8	11.9	5.82	7.93	4
20	34.8	284.4	2052.2	15.0	8.30	7.2	11
21	76.7	200.3	2229.5	19.4	6.23	6.6	17
22	21.4	274.4	2257.7	21.5	4.20	6.46	20
23	43.6	237.2	2185.4	18.5	6.21	6.72	20
24	57.4	300.7	2214.6	20.7	5.31	6.23	18
25	123.1	203.9	1993.3	9.9	9.23	7.64	21
26	195.5	276.5	2112.2	12.9	8.46	7.64	22

4. Results

Three sets of simulations were run with different parameter combinations. Following Mackay et al. (2003), an initial set of 2000 simulations were run for each of the 25 hillslopes with values for three canopy conductance parameters, g_{Smax} (range 17–126 mmol m^{-2} s^{-1}), Q_{min} (range 3000–9000 kJ m^{-2} day^{-1}), and δ (range 0.07–0.74 kPa^{-1}) randomly sampled from a naive (uniform) distribution. For this first set of simulations no parameters controlling available soil water were adjusted. Table 3 summarizes the average of these parameters taken from the ensemble of models retained using $|U(r) - \log_2 k|$ for the respective July and August TMS scenes. The Q_{min} averages are generally higher for August than for July, but no such clear pattern exists for g_{Smax} or δ. This indicates that there is a need for greater reduction in stomatal conductance for the August date

in comparison to July, and this reduction is not satisfied with a reduction in either g_{Smax} or δ. This is further evident in Fig. 4, which shows how stomatal sensitivity to D versus reference conductance for each hillslope compares to the theoretical universal line (Refer to Fig. 1) of stomatal regulation of leaf water potential (Oren et al., 1999). The figure clearly shows that the simulations for July are closely following the universal line. However, the simulations for August show considerable scatter, indicating that the simulation model is performing poorly when judged against the plant water-relations theory.

One hypothesis for the poor model performance for August is that soil moisture limitation is not adequately simulated. This reasoning would make sense if hillslopes at low elevation, with south-facing aspects and high leaf area index tended to follow the universal line the least. Fig. 5 shows a relationship between the calculated slope (m/G_{Sref}) and leaf area

Table 3
Summary of ensemble averages for the respective parameters for calibration with the July and August TMS images, respectively

Hillslope identifier	July			August		
	$E(Q_{min})$ (kJ m^{-2} day^{-1})	$E(G_{Smax})$ (mmol m^{-2} s^{-1})	$E(\delta)$ ((kPa)$^{-1}$)	$E(Q_{min})$ (kJ m^{-2} day^{-1})	$E(G_{Smax})$ (mmol m^{-2} s^{-1})	$E(\delta)$ ((kPa)$^{-1}$)
1	6565.0	85.8	0.433	5449.6	99.1	0.540
2	5641.0	73.8	0.410	5827.2	72.0	0.401
3	6305.2	80.0	0.411	7182.0	74.4	0.466
4	5639.8	75.9	0.420	6269.5	71.9	0.489
5	5892.9	73.2	0.389	6086.8	72.4	0.465
6	4890.0	43.9	0.359	5055.3	89.3	0.411
7	5823.0	68.6	0.428	7221.1	75.7	0.452
8	3588.6	61.0	0.406	5630.6	82.0	0.409
9	6689.6	67.4	0.433	6376.3	88.0	0.421
10	5798.1	71.3	0.403	6866.2	102.3	0.384
12	6655.6	61.4	0.442	3809.2	81.5	0.305
13	3561.4	41.9	0.413	7721.5	80.0	0.454
14	4910.7	54.8	0.442	7631.9	81.0	0.516
15	4112.3	60.7	0.411	5207.2	65.2	0.348
16	6006.6	80.8	0.402	6891.3	81.0	0.447
17	5503.4	69.1	0.412	5748.1	64.2	0.412
18	5558.6	71.4	0.417	5288.4	65.2	0.397
19	4738.1	44.6	0.413	4923.1	76.7	0.349
20	3460.6	66.8	0.406	3798.1	75.8	0.391
21	5353.8	81.2	0.432	5094.9	71.3	0.439
22	5475.0	84.6	0.396	5508.0	84.6	0.410
23	5451.5	77.1	0.394	5233.5	66.5	0.394
24	5371.6	81.9	0.416	5537.8	83.8	0.402
25	4010.8	43.5	0.420	6989.5	71.7	0.497
26	3917.9	59.3	0.415	6842.6	75.0	0.449
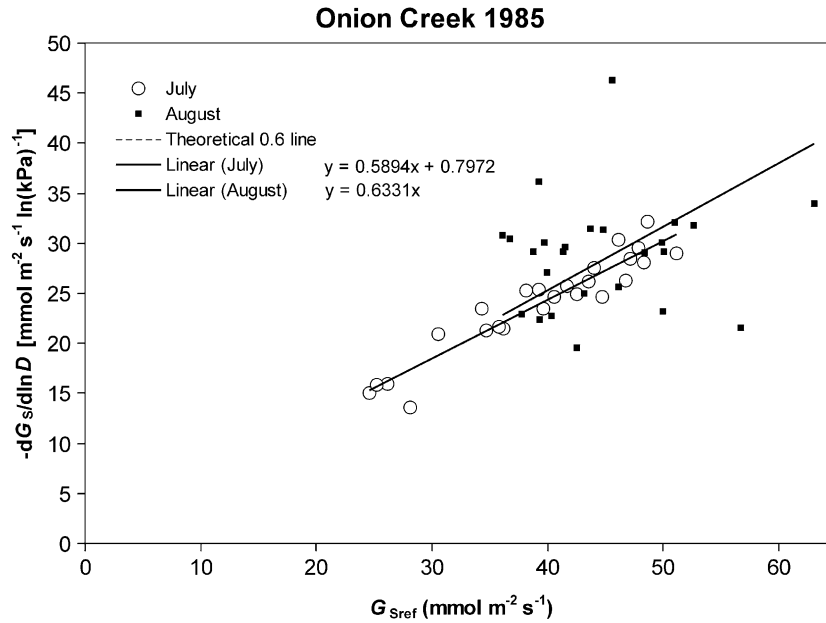
Fig. 4. These plots show the relationships between stomatal sensitivity to vapor pressure deficit and reference conductance at a vapor pressure deficit of 1 kPa for all hillslopes for both July and August TMS scene dates. The dashed line has a slope $0.6 \ln (kPa)^{-1}$, which has been shown by a large volume of data and modeling to represent a universal tradeoff in stomatal function (Oren et al., 1999; Ewers et al., 2000). Plants that regulate their water potential to just prevent runaway cavitation should theoretically fall on this line. The solid lines represent linear regressions for the July and August points, respectively. For the August plots the regression line was forced through the origin, since we expect stomatal sensitivity to be zero at full stomatal closure. Note that both fitted lines have slope near the theoretical 0.6 line, and in particular the July result shows a strong fit ($R^2 = 0.89$).

index, L, for the hillslopes organized into three groups by elevation. At low elevation, high evaporative demand, sites there is a strong positive relationship between the m/G_{Sref} and L. This relationship is weaker at the intermediate elevations and non-existent at the high elevations. Where m/G_{Sref} is near 0.6 indicates that the simulations are consistent with the universal line. When m/G_{Sref} exceeds 0.6 this indicates δ is increasing to compensate for an underestimated soil moisture stress or too low Q_{min}. At values below 0.6 it is possible that simulated soil moisture stress is too great. While this result supports the notion that soil moisture limits are poorly represented in the simulations, it does not fully explain why Q_{min} increases for August. Fig. 6 shows a positive relationship between m/G_{Sref} and Q_{min}. In addition, the position of each hillslope (above or below $m/G_{Sref} = 0.6$) can be explained in terms of properties that affect water supply versus demand. Lower elevation hillslopes and a steep, southwest aspect hillslope have $m/G_{Sref} \gg 0.6$ and correspondingly higher Q_{min}. This indicates that
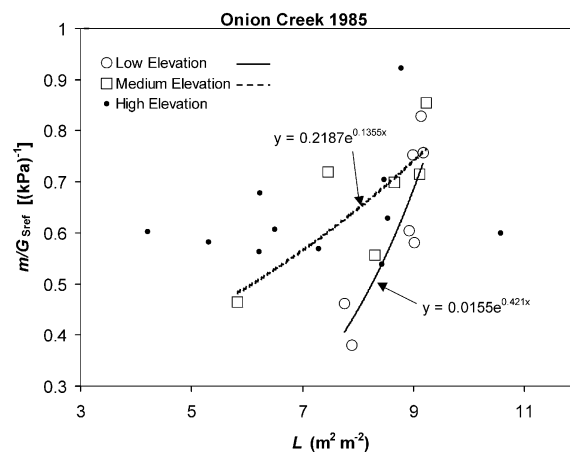
Fig. 5. Shown in this figure are relations between m/G_{Sref}, which theory suggests should have a value of 0.6, and leaf area index (L). The hillslopes have been sorted by their average elevation into low, medium and high categories to show that at lower elevations where temperatures are higher there is a relatively strong correspondence between the m/G_{Sref} and L. This relationship is not significant at the high elevations at which most of the hillslopes follow the theory.
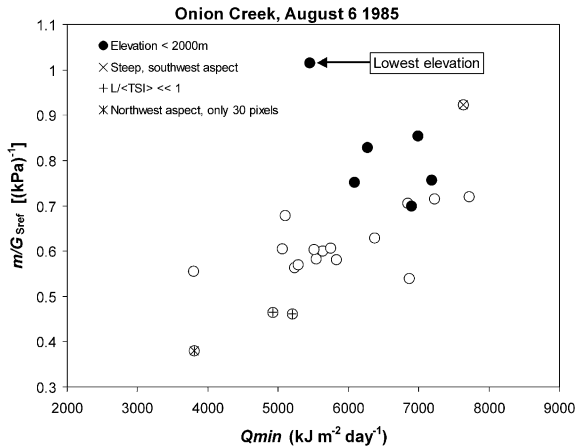
Fig. 6. Shown in this figure are relations between m/G_{Sref}, which theory suggests should have a value of 0.6, and Q_{min}. It shows a clear positive relationship that suggests that Q_{min} is compensating for factors controlling stomata that are not represented properly in the model, such as pre-dawn soil water potential. Individual hillslopes and groups of hillslopes, which do not follow water regulation theory ($m/G_{Sref} = 0.6$) are distinguished in terms of low elevation or high radiation load (steep, southwest aspect) for greater than expected apparent stomatal regulation of water potential, and low moisture demand versus supply ($L/\langle TSI \rangle \ll 1$) or northwest aspect for lower than expected apparent stomatal regulation of water potential.

areas of higher moisture demand for the amount of supply are simulated as too wet, which forces the canopy parameters to compensate by exceeding the universal line. Hillslopes with low L per unit $\langle TSI_h \rangle$ (an index of water demand versus supply) or northwest aspect have $m/G_{Sref} \ll 0.6$ and lower Q_{min} values. These hillslopes are simulated as having too little soil moisture, which requires the canopy parameters to compensate by falling below the universal line.

It appears that Q_{min} is being used incorrectly to compensate for a poor representation of soil water limitation on stomatal conductance. Since it is a surrogate for the light limitation on stomatal opening, which is species dependent, there is no clear justification for changing Q_{min} between July and August. To remedy this a second set of 2000 simulations per hillslope was run using a single Q_{min} of 5237 kJ m^{-2} day^{-1} determined as the average July Q_{min} for all hillslopes, and the rooting length parameter, R'_h, was randomly sampled from an uninformed distribution with a range of 0.01–0.1 m.

The results are shown in Fig. 7. Overall, there is a substantial improvement in the fit of each hillslope to the universal line for both dates. The August date still shows more scatter. Based on the inset plot in Fig. 7 there is a strong, positive relationship between m/G_{Sref} and the rooting length. This relationship is similar to the one shown in Fig. 6, indicating a tradeoff is occurring between R'_h and Q_{min}. To test this hypothesis, a third and final set of 2000 simulations was run using the ensemble average July Q_{min} values from Table 3, for the respective hillslopes. The results are shown in Fig. 8. The results show a tight clustering of all hillslopes on the universal line, but at a narrow range of G_{Sref}. Furthermore, R'_h, shown inset in Fig. 8, now has a narrow range of values, which means all hillslopes are converging to a point in parameter space.

5. Discussion

The parameter tradeoffs (g_{Smax} versus δ) seen in the daily simulations of transpiration suggest that the Jarvis model captures stomatal regulation of water potential. The tradeoffs seen with this relatively coarse simulation with sparse data are consistent with those proposed in theory (Monteith, 1995), extensively tested against a large amount of porometry and sap flux data (Oren et al., 1999), and obtained using a half-hourly model driven by in situ micrometeorology and calibrated with sap flux data (Mackay et al., 2003). It is important to realize that, without this direct comparison to water-relations theory, it is possible that numerous factors would have contributed to this apparent physically consistent behavior of the model. For example, there are abundant degrees of freedom given the uncertainties in both model inputs and in deriving surface temperature from TMS. Furthermore, one should be cautious in interpreting simulation model parameters obtained from ensemble averages. The values for the respective parameters may simply approach the mean of the a priori distributions from which they are sampled. This problem can be avoided by applying an iterative refinement of the parameter values, as was done in this paper. The fact that a large range of G_{Sref} is obtained for the first and second set of simulations (Figs. 4 and 7) is proof that parameter values for each
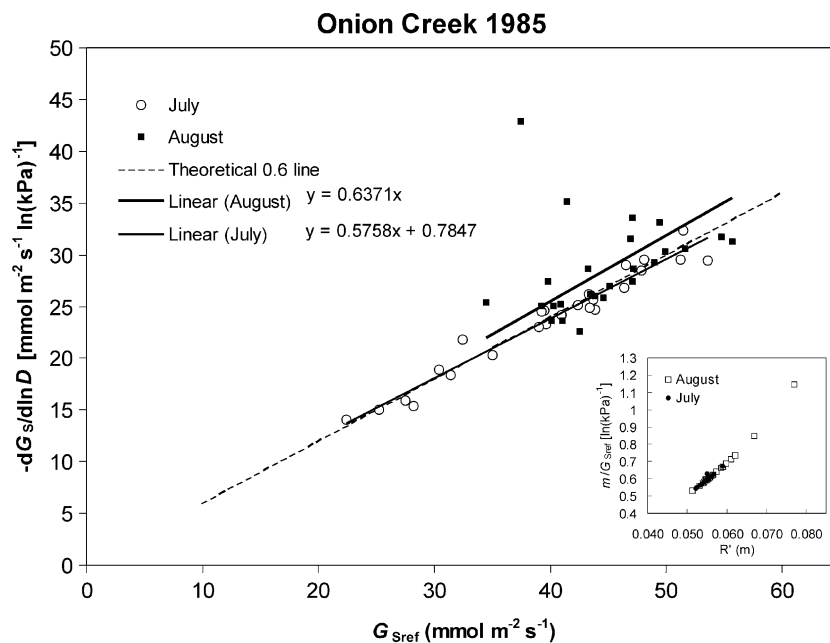
Fig. 7. These plots show the relationships between stomatal sensitivity to vapor pressure deficit and reference conductance at a vapor pressure deficit of 1 kPa for all hillslopes for both July and August TMS scene dates. This result is from the second set of simulations in which the rooting length scalar, R', is varied. The dashed line has a slope 0.6 ln $(kPa)^{-1}$, which has been shown by a large volume of data and modeling to represent a universal tradeoff in stomatal function (Oren et al., 1999; Ewers et al., 2000). Plants that regulate their water potential to just prevent runaway cavitation should theoretically fall on this line. The solid lines represent linear regressions for the July and August points, respectively. For the August plots the regression line was forced through the origin, since we expect stomatal sensitivity to be zero at full stomatal closure. Note that both fitted lines have slope near the theoretical 0.6 line, and in particular the July result shows a strong fit ($R^2 = 0.95$). August has a good fit for all except two hillslopes. Inset plots show relationships between m/G_{Sref} and the rooting length scalar.

hillslope are not simply taking on the distribution means for the respective parameters. Instead, the results show that by following water-relations theory a progressive refinement of the Jarvis-type model parameters is obtained.

The progressive refinement of model parameter values demonstrates an important distinction between automated versus knowledge-based parameterization schemes. Automated schemes (Binley and Beven, 1991; Gupta et al., 1998; Samanta and Mackay, 2003) tend to be naïve and extremely sensitive to the type of objective functions used, as would be the case in the present paper. Knowledge-based schemes are sensitive to the application domain (Franks and Beven, 1997; Boyle et al., 2000; Mackay et al., 2003), take into consideration intuition about the function of the modeled system, and tend to be less sensitive to specific objective functions. The universal line (Oren et al., 1999) summarizes a large amount of data on

plant hydraulic function. Based on the results in this paper for watershed-scale modeling and those of Mackay et al. (2003) for stand-level modeling, there is sufficient justification for the argument that the Jarvis model parameters can be made to follow the universal line. This does not confirm that the models mimic plant hydraulic function, anymore than it confirms a direct correspondence between predicted stomatal conductance rates and what might be observed through more direct methods, such as sap flux. It does suggest the hypothesis that the combination of simulation model and thermal remote sensing data used in this paper with the particular data set is sensitive to the same tradeoffs in stomatal regulation of leaf water potential that is more directly quantifiable with sap flux. A study that combines ground validation, including sap flux, combined with thermal remote sensing data should be able to test this hypothesis.
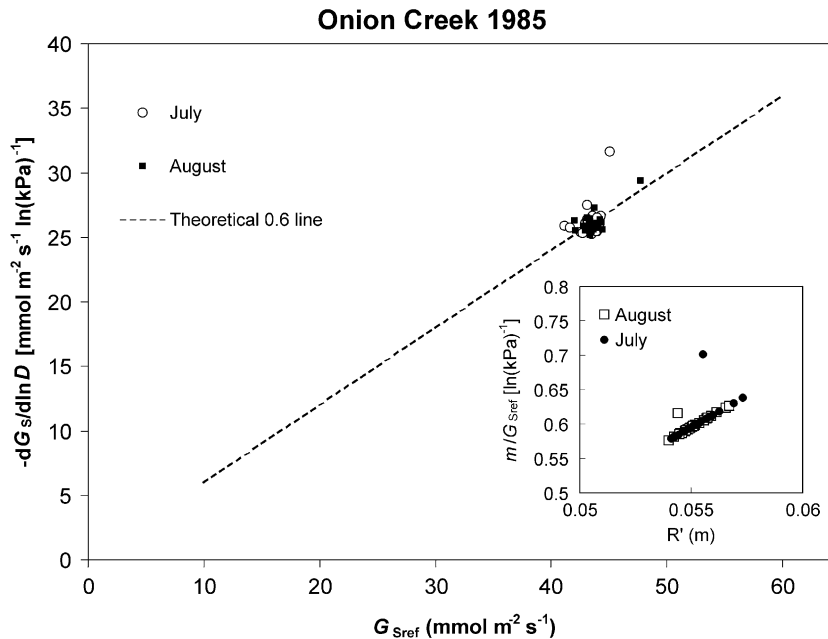
Fig. 8. These plots show the relationships between stomatal sensitivity to vapor pressure deficit and reference conductance at a vapor pressure deficit of 1 kPa for all hillslopes for both July and August TMS scene dates. This result is from the third set of simulations in which the rooting length scalar, R', is varied, and Q_{min} is derived from the July ensembles for the first set of simulations. The dashed line has a slope 0.6 ln $(kPa)^{-1}$, which has been shown by a large volume of data and modeling to represent a universal tradeoff in stomatal function (Oren et al., 1999; Ewers et al., 2000). Plants that regulate their water potential to just prevent runaway cavitation should theoretically fall on this line. Inset plots show relationships between m/G_{Sref} and the rooting length scalar.

The results suggest that the four parameters, g_{Smax}, δ, Q_{min}, and R'_h are sufficient for parameterizing the Jarvis model within RHESSys applied to conifer-covered watersheds. Among hillslope variations in Q_{min} and rooting depths or some similar proxy of available soil moisture appear to explain much of the variation among hillslopes. Once these are accounted for, g_{Smax} and δ parameters can be identified and are nearly equal for all hillslopes. While this is not necessarily representative of individual locations within the watershed, the average values of maximum stomatal conductance obtained are typical for conifer canopies (Running and Coughlan, 1988; Kelliher et al., 1995). This suggests that, at a scale of hillslopes or larger, average canopy parameters are acceptable, at least for the conifer biome. While this approach used to calibrate RHESSys does not resolve within-hillslope details in canopy parameters, it does allow for an assessment of physically meaningful parameter tradeoffs. The tradeoffs between canopy parameters indicate a physiological basis for interpreting

simulated transpiration. Based on the universal line transpiration rates are reduced either by lowering G_{Sref} or by increasing m. To prevent runaway cavitation a plant either needs to have a low set point for its leaf water potential, which requires a high structural integrity of its cell walls (or low vulnerability to cavitation), or it must safeguard against high leaf water potentials by closing stomata. On one hand, the 'efficiency' associated with a high G_{Sref} comes at a cost, as high K_L per unit L is needed to meet the high demand for water, and this makes the plant vulnerable to hydraulic failure (Ewers et al., 2000). On the other hand, the 'safety' associated with a low G_{Sref} means the plant can have a lower K_L per unit L. While this reduces its vulnerability to hydraulic failure when water is limiting or atmospheric demand for water is high it also compromises the photosynthetic capacity when water supply exceeds demand. This has direct implications for carbon gain and plant growth. The simulation model mimics this by either reducing g_{Smax} or increasing δ. A higher g_{Smax} allows a simulated

plant to take advantage of optimal environmental conditions to maximize CO_2 gain. These differences in stomatal response to environmental factors have important implications for land surface process modeling of water and carbon exchange, from short to long timescales. The safety versus efficiency tradeoffs embodied provides a direct physical connection between model parameterization and the physiological functioning of vegetation at watershed scales. As such, this model could be considered complimentary to the traditional land surface parameterization schemes based on biome classification coupled with remote sensing (Running et al., 1995; Sellers et al., 1996; Zeng et al., 2000). Parameterization of the variability in canopy physiology at large scales then amounts to mapping the land surface into positions along the continuum between safe and efficient strategies. This could greatly simplify the task of quantifying surface resistances over large regions.

A major challenge in parameterizing surface resistance parameters from remote sensing is the typical low signal-to-noise ratio. This has lead to the use of thermal inertia (Anderson et al., 1997; Norman et al., 2000) and empirical relations between vegetation vigor and surface temperature (Nemani and Running, 1989; Carlson et al., 1995) to effectively separate information from noise. The approach in this paper is similar in that an empirical relationship between reference conductance and stomatal sensitivity to water loss is used to distinguish between signal and noise. The approach is similar to that of Franks and Beven (1997) in that spatial variation in surface temperature is used to constrain the identification of model parameters. A physical interpretation in that paper relied on strong gradients in vegetation types (grass versus gallery forest). The present paper takes this type of analysis a significant step towards finding a direct physical interpretation of parameters in terms of the hydraulic functioning of the vegetation. This can resolve gradients in physiological functioning even when taxonomic classification is highly aggregated, as is typically the case for remote sensing data. The results suggest a potential refinement of current remote sensing algorithms to include the universal line describing the regulation of leaf water potential. This would improve future estimates of land surface parameters, particularly for forests

where strong gradients in surface temperature do not necessarily accompany strong gradients in water flux.

6. Conclusions

A Jarvis-type model of stomatal conductance can be reliably parameterized at a daily time scale in a meso-scale watershed with a limited amount of thermal remote sensing imagery. However, parameter values need to be determined carefully, as there are numerous compensations among parameters. The key strength of the approach applied in this paper is that parameter values are not chosen strictly based on degree of fit between the simulated latent heat fluxes and the surface temperatures obtained from the thermal remote sensing data. Instead, a set of simulation results that cannot be rejected based on their information content is used as an ensemble. Furthermore, the ensemble parameter values are compared against water-relations theory, which lends a direct physical interpretation to the estimated parameters. The results are in agreement with those obtained in other studies of direct analysis of leaf-level porometry measurements, whole-tree sap flux measurements, and whole canopy modeling validated with sap flux measurements. While further work is needed to assess the reliability of the approach across a range of biomes, it appears to provide a direct link between estimating stomatal conductance from remote sensing data and more direct ground observations of plant water-relations.

References

Aber, J.D., Federer, C.A., 1992. A generalized, lumped-parameter model of photosynthesis, evapotranspiration and net primary production in temperate and boreal forest ecosystems. Oecologia 92, 463–474.

Anderson, M.C., Norman, J.M., Diak, G.R., Kustas, W.P., 1997. A two-source integrated model for estimating surface fluxes for thermal infrared satellite observations. Remote Sensing of Environment 60, 195–216.

Ball, J.T., Woodrow, I.E., Berry, J.A., 1987. A model predicting stomatal conductance and its contribution to the control of photosynthesis under different environmental conditions. In: Biggens, J., (Ed.), Progress in Photosynthesis Research, vol. 4. Martinus Nijhoff Publishers, Dordrecht, the Netherlands, pp. 221–229.

Band, L.E., Patterson, P., Nemani, R., Running, S.W., 1993. Forest ecosystem processes at the watershed scale: incorporating hillslope hydrology. Agricultural and Forest Meteorology 63, 93–126.

Band, L.E., Mackay, D.S., Creed, I., Semkin, R., Jeffries, D.S., 1996. Ecosystem processes at the watershed scale: sensitivity to potential climate change. Limnology and Oceanography 41 (5), 928–938.

Baron, J.S., Hartman, M.D., Band, L.E., Lammers, R.B., 2000. Sensitivity of a high elevation Rocky Mountain watershed to altered climate and CO_2. Water Resources Research 36 (1), 89–99.

Bastiaanssen, W.G.M., Menenti, M., Feddes, R.A., Holtslag, A.A.M., 1998. A remote sensing surface energy balance algorithm for land (SEBAL). 1. Formulation. Journal of Hydrology 212/213, 198–212.

Beven, K., 1986. Runoff production and flood frequency in catchments of order n: an alternative approach. In: Gupta, V.K., Rodriguez-Iturbe, I., Wood, E.F. (Eds.), Scale Problems in Hydrology, D. Reidel Publishing Co, Dordrecht, pp. 107–131.

Beven, K.J., Binley, A., 1992. The future of distributed models: model calibration and uncertainty prediction. Hydrological Processes 6, 279–298.

Beven, K.J., Kirkby, M.J., 1979. A physically based, variable contributing area model of basin hydrology. Hydrological Sciences Bulletin 1, 43–69.

Binley, A.M., Beven, K.J., 1991. Physically-based modeling of catchment hydrology: a likelihood approach to reducing predictive uncertainty. In: Farmer, D.J., Rycroft, M.J. (Eds.), Computer Modelling in the Environmental Sciences, IMA Conference Series, Clarendon Press, Oxford, pp. 75–88.

Boyle, D.P., Gupta, H.V., Sorooshian, S., 2000. Toward improved calibration of hydrologic models: combining the strengths of manual and automated methods. Water Resources Research 36 (12), 3663–3674.

Brooks, R.H., Corey, A.T., 1964. Hydraulic Properties of Porous Media, Hydrologic Paper 3, Colorado State University, Fort Collins, p. 27.

Carlson, T.N., Capehart, W.J., Gillies, R.R., 1995. A new look at the simplified method for remote sensing of daily evapotranspiration. Remote Sensing of Environment 54, 161–167.

Crago, R.D., 1996. Conservation and variability of the evaporative fraction during the daytime. Journal of Hydrology 180, 173–194.

Crago, R.D., Brutsaert, W., 1996. Daytime evaporation and self-preservation of the evaporative fraction and the Bowen ratio. Journal of Hydrology 178, 241–255.

Creed, I.F., Band, L.E., Foster, N.W., Morrison, I.K., Nicolson, J.A., Semkin, R.S., Jeffries, D.S., 1996. Regulation of nitrate-N release from temperate forests: a test of the N flushing hypothesis. Water Resources Research 32 (11), 3337–3354.

Ewers, B.E., Oren, R., Sperry, J.S., 2000. Influence of nutrient versus water supply on hydraulic architecture and water balance in *Pinus taeda*. Plant, Cell and Environment 23, 1055–1066.

Ewers, B.E., Oren, R., Johnsen, K.H., Landsberg, J.J., 2001. Estimating maximum mean canopy stomatal conductance for use in models. Canadian Journal of Forest Research 31, 198–207.

Famiglietti, J.S., Wood, E.F., 1994. Multi-scale modeling of spatially-variable water and energy balance processes. Water Resources Research 30, 3061–3078.

Foley, J.A., Prentice, I.C., Ramankutty, N., Levis, S., Pollard, D., Sitch, S., Haxeltine, A., 1996. An integrated biosphere model of land surface processes, terrestrial carbon balance, and vegetation dynamics. Global Biogeochemical Cycles 10 (4), 603–628.

Foley, J.A., Levis, S., Costa, M.H., Cramer, W., Pollard, D., 2000. Incorporating dynamic vegetation cover within global climate models. Ecological Applications 10 (6), 1620–1632.

Franks, S., Beven, K.J., 1997. Estimation of evapotranspiration at the landscape scale: a fuzzy disaggregation approach. Water Resources Research 33 (12), 2929–2938.

van Genuchten, M.Th., 1980. A closed-form equation for predicting the hydraulic conductivity of unsaturated soils. Soils Science Society of America Journal 44, 892–898.

Gholtz, H.L., 1982. Environmental limits on aboveground net primary production, leaf area, and biomass in vegetation zones of the pacific northwest. Ecology 63 (2), 469–481.

Goward, S.N., Cruickshanks, G.D., Hope, A.S., 1985. Observed relation between thermal emission and reflected spectral radiance of a complex vegetation landscape. Remote Sensing of Environment 18, 137–146.

Grier, C.C., Running, S.W., 1977. Leaf area of mature northwestern coniferous forests: relation to site water balance. Ecology 58, 893–899.

Gupta, H.V., Sorooshian, S., Yapo, P.O., 1998. Towards improved calibration of hydrologic models: multiple and non-commensurable measures of information. Water Resources Research 34 (4), 751–763.

Hartley, R.V.L., 1928. Transmission of information. The Bell Systems Technical Journal 7 (3), 535–563.

Higashi, M., Klir, G.J., 1982. On measures of fuzziness and fuzzy complements. International Journal of General Systems 8 (3), 169–180.

Holbo, H.R., Luvall, J.C., 1989. Modeling surface temperature distributions in forest landscapes. Remote Sensing of Environment 27, 11–24.

Idso, S.B., Reginato, R.J., Jackson, R.D., 1978. An equation for potential evaporation from soil, water and crop surfaces

adaptable to use by remote sensing. Geophysical Research Letters 4, 187–188.

Jackson, R.D., Idso, S.B., Reginato, R.J., Pinter, P.J. Jr., 1981. Canopy temperature as a crop water stress indicator. Water Resources Research 17, 1133–1138.

Jarvis, P.G., 1976. The interpretation of the variations in leaf water potential and stomatal conductance found in canopies in the field. Philosophical Transactions of the Royal Society of London, Series B 273, 593–610.

Jarvis, P.G., 1980. Stomatal response to water stress in conifers. In: Turner, N.C., Kramer, P.J. (Eds.), Adaptation of Plants to Water and High Temperature Stress, Wiley, New York, pp. 105–122.

Kelliher, F.M., Leuning, R., Raupach, M.R., Schulze, E.-D., 1995. Maximum conductances for evaporation from global vegetation types. Agricultural and Forest Meteorology 73, 1–16.

Klepper, O., Scholten, H., Van De Kamer, J.P.G., 1991. Prediction uncertainty in an ecological model of the Oosterschelde Estuary. Journal of Forecasting 10, 191–209.

Klir, G.J., Wierman, M.J., 1998. Uncertainty-Based Information: Elements of Generalized Information Theory, Physica-Verlag, Heidelberg.

Kuczera, G., 1982. On the relationship between the reliability of parameter estimates and hydrologic time series data used in calibration. Water Resources Research 18 (1), 146–154.

Kuczera, G., 1983. Improved parameter inference in catchment models. 2. Combining different kinds of hydrologic data and testing their compatibility. Water Resources Research 19 (5), 1163–1172.

Kuczera, G., Parent, E., 1998. Monte Carlo assessment of parameter uncertainty in conceptual catchment models: the Metropolis algorithm. Journal of Hydrology 211, 69–85.

Kustas, W.P., Perry, E.M., Doraiswamy, P.C., Moran, M.S., 1994. Using satellite remote sensing to extrapolate evapotranspiration estimates in time and space over a semiarid rangeland basin. Remote Sensing of Environment 49, 275–286.

Larcher, W., 1995. Physiological Plant Ecology, 3rd ed, Springer, Berlin.

Leuning, R., Kelliher, F.M., De Pury, D.G.G., Schulze, E.-D., 1995. Leaf nitrogen, photosynthesis, conductance and transpiration: scaling from leaves to canopies. Plant, Cell and Environment 18, 1183–1200.

Liang, C., Mackay, D.S., 2000. A general model of watershed extraction and representation using globally optimal flow paths and up-slope contributing areas. International Journal of Geographical Information Science 14 (4), 337–358.

Lohammar, T., Larsson, S., Linder, S., Falk, S.O., 1980. FAST-simulation models of gaseous exchange in Scots pine. Ecological Bulletin 32, 505–523.

MacDonald, L.H., 1986. Persistence of Soil Moisture Changes Resulting from Artificially Extended Snowmelt, Proceedings of the Western Snow Conference, Phoenix, AZ, April 15–17, 1985, Colorado State University Press, Fort Collins, pp. 146–149.

MacDonald, L.H., 1987. Forest harvest, snowmelt and streamflow in the Central Sierra Nevada. Forest Hydrology and Watershed Management (Proceedings of the Vancouver Symposium, August, 1987), 273–283.

MacDonald, L.H., 1989. Snowmelt and Streamflow in the Central Sierra Nevada: Effects of Forest Harvest and Cloud-Seeding. Unpublished PhD Dissertation, Department of Forestry and Resource Management, University of California, Berkeley.

Mackay, D.S., 2001. Evaluation of hydrologic equilibrium in a mountainous watershed: incorporating forest canopy spatial adjustment to soil biogeochemical processes. Advances in Water Resources 24 (9–10), 1211–1227.

Mackay, D.S., Band, L.E., 1997. Forest ecosystem processes at the watershed scale: dynamic coupling of distributed hydrology and canopy growth. Hydrological Processes 11, 1197–1217.

Mackay, D.S., Robinson, V.B., 2000. A multiple criteria decision support system for testing integrated environmental models. Fuzzy Sets and Systems 113, 53–67.

Mackay, D.S., Ahl, D.E., Ewers, B.E., Samanta, S., Gower, S.T., Burrows, S.N., 2003. Physiological tradeoffs in the parameterization of a model of canopy transpiration. Advances in Water Resources 26 (2), 179–194.

McNaughton, K.G., Jarvis, P.G., 1991. Effects of spatial scale on stomatal control of tranpiration. Agricultural and Forest Meteorology 54, 279–301.

Melching, C.S., 1995. In: Singh, V.P., (Ed.), Reliability Estimation in Computer Models of Watershed Hydrology, Water Resources Publication, Highlands Ranch, CO, pp. 69–118.

Monteith, J.L., 1965. Evaporation and Environment, Proceedings of the 19th Symposium of the Society for Experimental Biology, Cambridge University Press, New York, pp. 205–233.

Monteith, J.L., 1995. A reinterpretation of stomatal response to humidity. Plant, Cell and Environment 18, 357–364.

Nemani, R.R., Running, S.W., 1989. Estimation of regional surface resistance to evapotranspiration from NDVI and thermal-IR AVHRR data. Journal of Applied Meteorology 28 (4), 276–284.

Nemani, R., Pierce, L., Running, S., Band, L., 1993. Forest ecosystem processes at the watershed scale: sensitivity to remotely-sensed leaf area index estimates. International Journal of Remote Sensing 14 (13), 2519–2534.

Norman, J.M., Kustas, W.P., Prueger, J.H., Diak, G.R., 2000. Surface flux estimation using radiometric temperature: a dual-temperature-difference method to minimize measurement errors. Water Resources Research 36 (8), 2263–2274.

Oren, R., Sperry, J.S., Katul, G.G., Pataki, D.E., Ewers, B.E., Phillips, N., Schafer, K.V.R., 1999. Survey and synthesis of intra- and interspecific variation in stomatal sensitivity to vapour pressure deficit. Plant, Cell and Environment 22, 1515–1526.

Oreskes, N., Shrader-Frechette, K., Belitz, K., 1994. Verification, validation, and confirmation of numerical models in the earth sciences. Science 263, 641–646.

Pierce, L.L., Congalton, R.G., 1988. A methodology for mapping forest latent heat flux densities using remote sensing. Remote Sensing of Environment 24, 405–418.

Quinn, P., Beven, K., Lamb, R., 1995. The ln(a/tan B) index: how to calculate it and how to use is within the TOPMODEL framework. Hydrological Processes 9, 161–182.

Running, S.W., Coughlan, J.C., 1988. A general model of forest ecosystem processes for regional applications. I. Hydrologic

balance, canopy gas exchange and primary production processes. Ecological Modeling 42, 125–154.

Running, S.W., Hunt, E.R. Jr., 1993. Generalization of a forest ecosystem process model for other biomes, BIOME-BGC, and application for global scale models. In: Ehleringer, J.R., Field, C.B. (Eds.), Scaling Physiological Processes: Leaf to Globe, Academic Press, San Diego, CA, pp. 141–158.

Running, S.W., Loveland, T.R., Pierce, L.L., Nemani, R.R., Hunt, E.R. Jr., 1995. A remote sensing based vegetation classification logic for global land cover analysis. Remote Sensing of Environment 51, 39–58.

Saliendra, N.Z., Sperry, J.S., Comstock, J.P., 1995. Influence of leaf water status on stomatal response to humidity, hydraulic conductance, and soil drought in *Betula occidentalis*. Planta 196, 357–366.

Samanta, S., Mackay, D.S., 2003. Flexible automated parameterization of hydrologic models using fuzzy logic. Water Resources Research 39 (1), 1009, doi: 10.1029/2002WR001349.

Seguin, B., Itier, B., 1983. Using midday surface temperature to estimate daily evaporation from satellite thermal IR data. International Journal of Remote Sensing 4, 371–383.

Sellers, P.J., Los, S.O., Tucker, C.J., Justice, C.O., Dazlich, D.A., Collatz, G.J., Randall, D.A., 1996. A revised land surface parameterization (SiB$_2$) for atmospheric GCMs. Part II. The generation of global fields of terrestrial biophysical parameters from satellite data. Journal of Climate 9, 676–705.

Sellers, P.J., Dickinson, R.E., Randall, D.A., Betts, A.K., Hall, F.G., Berry, J.A., Collatz, G.J., Denning, A.S., Mooney, H.A., Nobre, C.A., Sato, N., Field, C.B., Henderson-Sellers, A., 1997. Modeling the exchange of energy, water, and carbon between continents and the atmosphere. Science 275, 502–509.

Sivapalan, M., Beven, K., Wood, E.F., 1987. On hydrologic 2. A scaled model of storm runoff production. Water Resources Research 23, 2266–2278.

Sorooshian, S., Gupta, V.K., 1983. Automatic calibration of conceptual rainfall–runoff models: the question of parameter observability and uniqueness. Water Resources Research 19 (1), 251–259.

Spear, R.C., Hornberger, G.M., 1990. Eutrophication in Peel Inlet—II identification of critical uncertainty via generalized sensitivity analysis. Water Resources Research 14, 43–49.

Sperry, J.S., Adler, J.R., Campbell, G.S., Comstock, J.S., 1998. Hydraulic limitation of a flux and pressure in the soil–plant continuum: results from a model. Plant, Cell and Environment 21, 347–359.

van Stratten, G., Keesman, K.J., 1991. Uncertainty propagation and speculation in projective forecasts of environmental change: a lake-eutrophication example. Journal of Forecasting 10, 163–190.

Tague, C.L., Band, L.E., 2001. Evaluating explicit and implicit routing for watershed hydro-ecological models of forest hydrology at the small catchment scale. Hydrological Processes 15, 1415–1439.

Tyree, M.T., Ewers, F.E., 1991. The hydraulic architecture of trees and other woody plants. New Phytologist 119, 345–360.

Tyree, M.T., Sperry, J.S., 1988. Do woody plants operate near the point of catastrophic xylem dysfunction caused by dynamic water stress? Answers from a model. Plant Physiology 88, 574–580.

Vertessy, R.A., Hatton, T.J., Benyon, R.G., Dawes, W.R., 1996. Long-term growth and water balance predictions for a mountain ash (*Eucalyptus regnans*) for catchment subject to clear-felling and regeneration. Tree Physiology 16, 221–232.

Watson, G.R., Vertessy, R.A., Band, L.E., 1996. Distributed parameterization of a large scale water balance model for an Australian forested region. HydroGIS 96: Application of Geographic Information Systems in Hydrology and Water Resources Management (Proceedings of Vienna Conference, April 1996), IAHS Publication No. 235.

White, J.D., Running, S.W., Thornton, P.E., Keane, R.E., Ryan, K.C., Farge, D.B., Key, C.H., 1998. Assessing simulated ecosystem processes for climate variability research at Glacier National Park, USA. Ecological Applications 8 (3), 805–823.

Wigmosta, M.S., Vail, L.W., Lettenmaier, D.P., 1994. A distributed hydrology-vegetation model for complex terrain. Water Resources Research 30 (6), 1665–1679.

Yapo, P.O., Gupta, H.V., Sorooshian, S., 1998. Multi-objective global optimization for hydrologic models. Journal of Hydrology 204, 83–97.

Yong, J.W.H., Wong, S.C., Farquhar, G.D., 1997. Stomatal response to changes in vapour pressure difference between leaf and air. Plant, Cell and Environment 20, 1213–1216.

Zadeh, L.A., 1965. Fuzzy sets. Information and Control 8 (3), 338–353.

Zadeh, L.A., 1978. Fuzzy sets as a basis for a theory of possibilities. International Journal of Fuzzy Sets and Systems 1 (1), 3–28.

Zeng, X., Dickinson, R.E., Walker, A., Shaikh, M., DeFries, R.S., Qi, J., 2000. Derivation and evaluation of global 1-km fractional vegetation cover data for land modeling. Journal of Applied Meteorology 39, 826–839.

Zhu, A.-X., Mackay, D.S., 2001. Effects of spatial detail of soil information on watershed modeling. Journal of Hydrology 248, 54–77.